# Nucleation of $\alpha_1$-Antichymotrypsin Polymerization†

Damian C. Crowther,*,‡ Louise C. Serpell,§ Timothy R. Dafforn,|| Bibek Gooptu,|| and David A. Lomas||

*Neurology Unit, Department of Medicine, and Department of Haematology, University of Cambridge, Cambridge Institute for Medical Research, Wellcome Trust/MRC Building, Hills Road, Cambridge, CB2 2XY, United Kingdom*

*Received April 5, 2002; Revised Manuscript Received September 10, 2002*

ABSTRACT: Alpha$_1$-antichymotrypsin is an acute phase plasma protein and a member of the serpin superfamily. We show here that wildtype $\alpha_1$-antichymotrypsin forms polymers between the reactive center loop of one molecule and the $\beta$-sheet A of a second at a rate that is dependent on protein concentration and the temperature of the reaction. The rate of polymerization was accelerated by seeding with polymers of $\alpha_1$-antichymotrypsin and a complex of $\alpha_1$-antichymotrypsin with an exogenous reactive loop peptide but not with reactive loop cleaved $\alpha_1$-antichymotrypsin or with polymers of other members of the serpin superfamily. Sonication of $\alpha_1$-antichymotrypsin polymers markedly increased the efficacy of seeding such that polymers were able to form under physiological conditions. Taken together, these data provide the first demonstration that serpin polymerization can result from seeding. This mechanism is analogous to the fibrillization of the A$\beta_{1-42}$ peptide and may be important in the deposition of $\alpha_1$-antichymotrypsin in the plaques of Alzheimer's disease.

The A$\beta_{1-42}$ peptide and $\alpha_1$-antichymotrypsin are obligate components of amyloid plaques in Alzheimer's disease (*1*). Previous studies have demonstrated that the conformational change that precedes the tissue deposition of A$\beta_{1-42}$ is dependent upon nucleation (*2*). Nucleation dependent kinetics are characterized by an initial lag phase during which dimers or small oligomers form. Once the oligomers have formed then further polymerization of monomers occurs more rapidly. The characterization of nucleation is important as there is increasing evidence that oligomers are the pathological species in several neurological conditions including Alzheimer's (*3*) and Parkinson's disease (*4*, *5*). Despite the wealth of evidence that A$\beta_{1-42}$ spontaneously forms oligomers and polymers, little is known about the kinetics of polymerization of $\alpha_1$-antichymotrypsin.

Alpha$_1$-antichymotrypsin is a member of the serine proteinase inhibitor or serpin superfamily (*6*, *7*). Members of this family are found throughout vertebrates and in plants and viruses. They are characterized by sequence homology with $\alpha_1$-antitrypsin and a tertiary structure based on three $\beta$-sheets, nine $\alpha$-helices, and a mobile reactive center loop (*8*). Following docking with the target proteinase, the serpin inactivates the enzyme by translocating it to the lower pole of the molecule and crushing it against the base of the inhibitor (*9*). This remarkable mechanism is achieved by the mobile reactive loop snapping into $\beta$-sheet A in a movement that is analogous to a mousetrap after the mouse has taken the bait (*10*). The conformational transition is essential for the protein to act as a proteinase inhibitor but may be destabilized by point mutations (*11*). Such mutations favor the incorporation of the reactive loop of a second molecule to form a reactive loop:$\beta$-sheet A dimer (*12*−*14*). The dimer can then extend to form chains of polymers (Figure 1a,b). Polymer formation is recognized to underlie the deficiency of naturally occurring variants of the serpins: $\alpha_1$-antitrypsin (*15*−*17*), $\alpha_1$-antichymotrypsin (*18*), C1-inhibitor (*19*, *20*), and antithrombin (*21*, *22*) in association with cirrhosis, chronic obstructive pulmonary disease, angio-oedema, and thrombosis, respectively. Moreover, the same process has recently been described in a novel inclusion body dementia (familial encephalopathy with neuroserpin inclusion bodies or FENIB[1]) because of polymerization and tissue deposition of the neurone specific protein, neuroserpin (*23*−*25*).

We report here the kinetics of polymerization of wildtype $\alpha_1$-antichymotrypsin and show that it can be accelerated by seeding with polymers of $\alpha_1$-antichymotrypsin and by $\alpha_1$-antichymotrypsin complexed with an exogenous reactive loop peptide inserted in $\beta$-sheet A. This process occurs under physiological conditions and may be important in the deposition of $\alpha_1$-antichymotrypsin in plaques in patients with Alzheimer's disease.

## MATERIALS AND METHODS

*Materials*. *N*,*N*′-dimethyl-*N*-(iodoacetyl)-*N*′-(7-nitrobenz-2-oxa-1,3- diazol-4-yl) ethylenediamine (IANBD) was obtained from Molecular Probes Europe BV, Leiden, The Netherlands. NAP-10 gel filtration columns and the ECL

† This work was supported by the Wellcome Trust and the Medical Research Council (U.K.).

* Corresponding author. Tel: +44 1223 762818. Fax: +44 1223 336827. E-mail: dcc26@cam.ac.uk.

‡ Neurology Unit.

§ Department of Haematology.

|| Department of Medicine.

[1] FENIB, familial encephalopathy with neuroserpin inclusion bodies; IANBD, *N*,*N*′-dimethyl-*N*-(iodoacetyl)-*N*′-(7-nitrobenz-2-oxa-1,3-diazol-4-yl) ethylenediamine; PAGE, polyacrylamide gel electrophoresis; PBS, phosphate buffered saline; SDS, sodium dodecyl sulfate; PAI-1, plasminogen activator inhibitor 1.

10.1021/bi0259305 CCC: $25.00 
Published on Web 02/04/2003

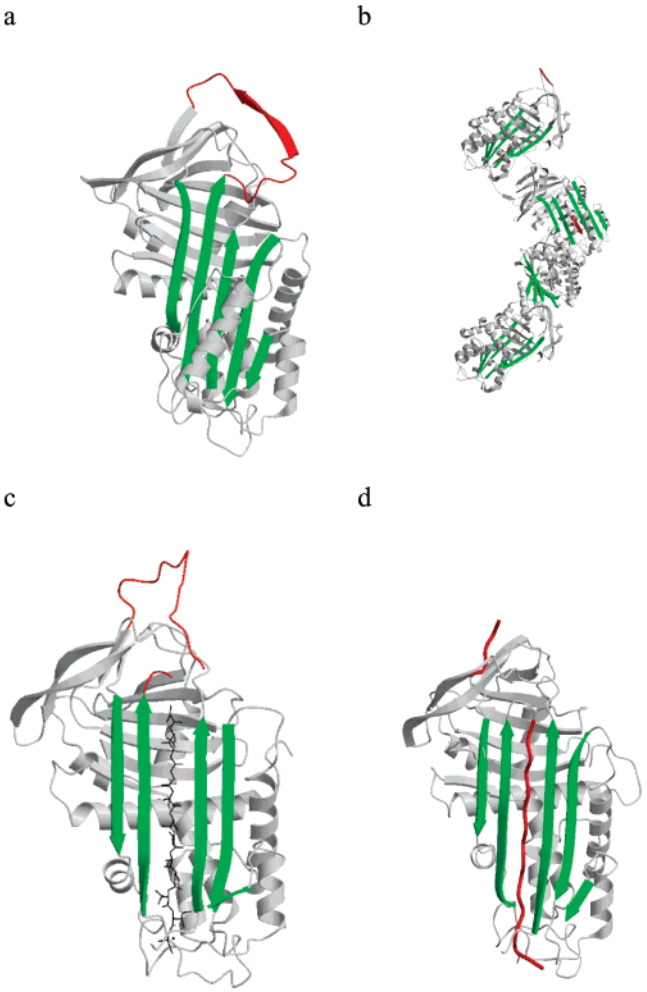


FIGURE 1: Conformers of the serpins. The native conformation of the serpins is typified by the crystal structure of $\alpha_1$-antitrypsin (Figure 1a, ref *16*). The model of the serpin polymer was constructed using biophysical analysis of the polymerization of $\alpha_1$-antitrypsin (Figure 1b, ref *14*). The structure of the serpin−peptide binary complex was determined for antithrombin complexed with a 12mer peptide corresponding to P14−P3 of the reactive center loop (Figure 1c, ref *50*). The reactive-loop-cleaved conformation of the serpins is exemplified by the crystal structure of cleaved $\alpha_1$-antitrypsin (Figure 1d, ref *51*). The reactive loop of each serpin molecule is shown in red, and $\beta$-sheet A is illustrated in green. In Figure 1c, the inserted peptide is shown as a ball-and-stick structure in the strand 4 groove of $\beta$-sheet A.

antigen detection kit were from Amersham Biosciences UK Ltd., Little Chalfont, U.K. Peroxidase-labeled goat anti-rabbit immunoglobulin and rabbit anti-$\alpha_1$-antichymotrypsin IgG were obtained from Dako Ltd., Ely, U.K. Ten nm-gold-conjugated anti-rabbit antibody was produced by British Biocell International and supplied by Agar Scientific Ltd., Stansted, U.K. Pioloform carbon coated copper mesh 400 grids for electron microscopy were from TAAB Laboratories Equipment Ltd., Aldermaston, U.K. All other materials were supplied by Sigma Chemical Company, Poole, U.K.

*Expression and Purification of Recombinant $\alpha_1$-Antichymotrypsin*. Recombinant wildtype $\alpha_1$-antichymotrypsin was expressed in the pzm-S plasmid in *Escherichia coli* N4830-1 with a temperature-sensitive promoter (*26*, *27*). The cells were lysed by sonication on ice, and $\alpha_1$-antichymotrypsin was purified by Q-Sepharose and DNA chromatography as described by Rubin and co-workers (*28*). The protein concentration was determined by Bradford assay; the inhibitory activity by titration against bovine α-chymotrypsin; and the purity by SDS, nondenaturing, and transverse urea gradient polyacrylamide gel electrophoresis (PAGE) (*29*). Reactive loop cleaved $\alpha_1$-antichymotrypsin was prepared by incubating the native protein at 1 mg/mL with 300:1 w/w porcine pancreatic trypsin for 1 h at room temperature. The proteinase was then inhibited with 4-(2-aminoethyl)-benzenesulfonyl fluoride (final concentration, 100 $\mu$M).

*Purification and Polymerization of Plasma $\alpha_1$-Antitrypsin and Antithrombin.* Alpha$_1$-antitrypsin and antithrombin were purified from plasma as detailed previously (*21*, *30*). Short chain polymers of $\alpha_1$-antitrypsin were prepared by heating purified $\alpha_1$-antitrypsin at 67 °C for 12 h in 0.7 M sodium citrate as detailed (*29*). Long chain polymers of $\alpha_1$-antitrypsin and antithrombin were prepared by heating the purified plasma serpins in 50 mM Tris and 50 mM KCl, pH 7.4, at 60 °C for 2 h.

*Fluorescent Labeling of $\alpha_1$-Antichymotrypsin*. IANBD was dissolved at 10 mg/mL in dimethyl sulfoxide. A 1.2 mg/mL solution of $\alpha_1$-antichymotrypsin in 50 mM Tris and 50 mM KCl, pH 7.4, was incubated with a 20-fold molar excess of IANBD for 18 h at 4 °C with gentle agitation. Labeled $\alpha_1$-antichymotrypsin was separated from unreacted IANBD and transferred into 50 mM Tris and 50 mM KCl, pH 7.4, by gel filtration using a G-25 column. This resulted in 100% specific labeling of the cysteine on $\alpha_1$-antichymotrypsin as determined from the $OD_{478}$ (extinction coefficient: 25 000 $cm^{-1}$ $M^{-1}$).

*Assessment of the Polymerization of $\alpha_1$-Antichymotrypsin*. Alpha$_1$-antichymotrypsin was polymerized by incubation at 200 $\mu$g/mL in 50 mM Tris and 50 mM KCl, pH 7.4, at 45 °C for 16 h. The progress of polymerization was monitored by visualizing 5 $\mu$g aliquots of protein on a 7.5−15% w/v nondenaturing PAGE. The rate of polymerization was also assessed by light scattering and intrinsic tryptophan fluorescence. Alpha$_1$-antichymotrypsin (300 $\mu$L) was incubated in a pre-warmed quartz cuvette (path length, 10 × 2 mm) in a thermostatically controlled cuvette holder. The solution was overlaid with 500 $\mu$L of mineral oil, and light scattering by the protein solution was assessed at 400 nm over $8 \times 10^4$ s in a Perkin-Elmer LS-50B spectrofluorimeter. The concentration of native $\alpha_1$-antichymotrypsin in the polymerization reaction ranged from 100 to 400 $\mu$g/mL, and the temperature of the reaction was varied between 37 and 50 °C. Intrinsic tryptophan fluorescence was assessed in an identical manner with an excitation wavelength of 295 nm and a detection wavelength of 340 nm (*13*). IANBD-labeled $\alpha_1$-antichymotrypsin was polymerized at concentrations between 10 and 400 $\mu$g/mL using the same conditions but was examined with an excitation wavelength of 478 nm and an emission wavelength of 541 nm. The slits controlling the intensity of the excitation light source were kept at the minimum machine-permissible limit of 2.5 nm; the emission slits were varied between 2.5 and 5 nm depending on the experimental conditions to give the optimal emission signal. For some experiments, $\alpha_1$-antichymotrypsin polymers were disrupted by sonication at 1 mg/mL in 50 mM Tris and 50 mM KCl, pH 7.4, on ice, using six cycles of sonication for 30 s followed by cooling for 30 s.

*Circular Dichroism (CD) Spectroscopy*. A JASCO J-810 spectropolarimeter was used to determine the CD spectra of

$\alpha_1$-antichymotrypsin at 200 $\mu$g/mL and 45 °C in 50 mM Tris and 50 mM KCl, pH 7.4, in a quartz cuvette with a path length of 1 mm. CD spectra were measured between 195 and 260 nm at intervals during a 24 h incubation. Protein concentration was assumed to remain constant throughout the incubation.

*Transmission Electron Microscopy and Immunogold Labeling of Polymers*. Four $\mu$L of polymeric $\alpha_1$-antichymotrypsin (200 $\mu$g/mL) were placed on pioloform carbon coated copper mesh 400 grids. The grid was blotted dry and placed on a blocking solution of 0.1% w/v gelatin in phosphate buffered saline (PBS). It was again blotted dry and then incubated for 1 h on a droplet of rabbit anti-$\alpha_1$-antichymotrypsin IgG diluted 1/200 in PBS. The grid was then washed 10 times with 0.1% w/v gelatin in PBS and placed on a droplet of 10 nm-gold-conjugated anti-rabbit antibody diluted 1/20 in gelatin (w/v) in PBS and incubated for 1 h. The grid was washed 10 times with 0.1% w/v gelatin in PBS and blotted dry. All grids were then negatively stained with a filtered 1% w/v solution of uranyl acetate in water and allowed to dry. The grids were examined using a Philips 208 electron microscope operating at 80 kV, and micrographs were taken at various magnifications (25 000−63 000×).

*Preparation of the Binary Complex between $\alpha_1$-Antichymotrypsin and an Exogenous Reactive Loop Peptide*. The binary complex was prepared by incubating $\alpha_1$-antichymotrypsin at 200 $\mu$g/mL in 50 mM Tris and 50 mM KCl, pH 7.4, at 37 °C with a 50-fold molar excess of a synthetic 12mer peptide that corresponds to P14−P3 of the reactive loop of antithrombin (Ac-Ser-Glu-Ala-Ala-Ala-Ser-Thr-Ala-Val-Val-Ile-Ala). The formation of the binary complex was monitored by assessing 5 $\mu$g aliquots of protein on 7.5−15% w/v nondenaturing PAGE. The residual peptide was removed by gel filtration on a G25 column equilibrated in 50 mM Tris and 50 mM KCl, pH 7.4.

## RESULTS

*Loop-Sheet Polymerization of $\alpha_1$-Antichymotrypsin*. Alpha$_1$-antichymotrypsin formed polymers when incubated at 200 $\mu$g/mL and 45 °C for 16 h (Figure 2a). During the course of the experiment, monomeric $\alpha_1$-antichymotrypsin was lost as the protein formed a ladder of slowly migrating, high molecular mass polymers. Negative staining with uranyl acetate revealed that the polymers were composed of linear filaments (Figure 2b) with occasional circular forms (Figure 2b, inset). These were confirmed to be $\alpha_1$-antichymotrypsin by immunogold labeling (data not shown). Examination of solutions of monomeric $\alpha_1$-antichymotrypsin by electron microscopy did not reveal any linear or circular species. Monomeric and polymeric $\alpha_1$-antichymotrypsin were then assessed by transverse urea gradient-PAGE. The monomeric protein had an unfolding transition that was typical for a serpin, but the polymeric bands were resistant to unfolding in 8 M urea (Figure 2c,d). Moreover, the polymeric species was inactive as an inhibitor of bovine $\alpha_1$-chymotrypsin and was resistant to reactive loop cleavage by porcine pancreatic trypsin, which cleaves between P5 and P4 (*31*). The formation of these inactive, stable, high molecular mass species is characteristic of the loop-sheet polymerization that has been reported in other members of the serpin superfamily (*13*, *32*, *33*).

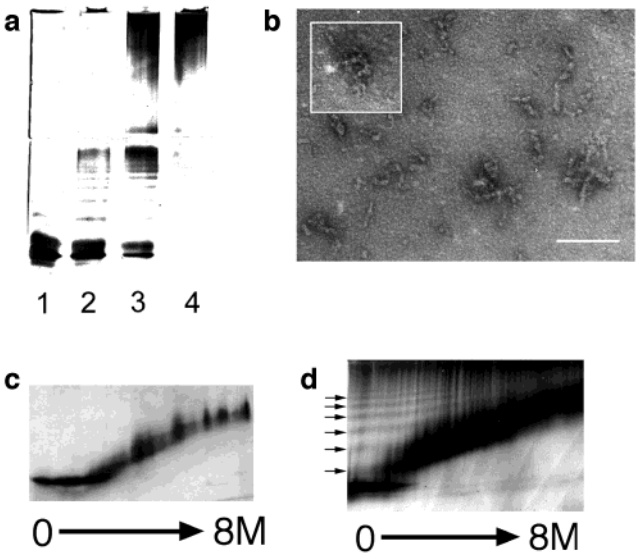


FIGURE 2: Nondenaturing PAGE (7.5−15% w/v) was used to assess the polymerization of $\alpha_1$-antichymotrypsin (Figure 2a). Native $\alpha_1$-antichymotrypsin (200 $\mu$g/mL in 50 mM Tris and 50 mM KCl, pH 7.4) was incubated at 45 °C for 0 (lane 1), 4 (lane 2), 8 (lane 3), and 16 h (lane 4). Each lane contained 10 $\mu$g of protein, and the bands were visualized by silver staining. Transmission electron microscopy demonstrated $\alpha_1$-antichymotrypsin polymers (Figure 2b, bar represents 100 nm) that were mostly linear with occasional circular species (Figure 2b, inset). Transverse urea gradient (TUG) gels (7.5% w/v) visualized the unfolding characteristics of native recombinant $\alpha_1$-antichymotrypsin (Figure 2c) and partially polymerized $\alpha_1$-antichymotrypsin (Figure 2d). Fifty (Figure 2c) and 100 $\mu$g (Figure 2d) of $\alpha_1$-antichymotrypsin were loaded on the TUG gels. Protein was visualized by silver staining, and the polymer bands are indicated with arrows.

*Spectroscopic Analysis of $\alpha_1$-Antichymotrypsin Polymerization*. The polymerization of $\alpha_1$-antichymotrypsin resulted in an increase in light scattering and a loss in the CD signal at 222 nm that mirrored the formation of polymers on nondenaturing PAGE (Figure 3a). Investigation of the concentration dependence of this CD change demonstrated a lag-phase at 200 and 400 $\mu$g/mL that was not apparent at 600 and 800 $\mu$g/mL. At 100 $\mu$g/mL, the signal was too noisy to detect a clear lag. CD spectra recorded before and after the polymerization reaction demonstrated changes in both $\alpha$-helical and $\beta$-sheet structure. Analysis using CONTILL and CDSSTR programs (from http://lamar.colostate.edu/~sreeram/CDPro/CDPro.htm) predicted a decrease in $\alpha$-helical content from 26% in monomers to 11% in polymers and an increase in $\beta$-sheet structure from 21% in monomers to 26% in polymers (Figure 3b). Reactive-loop cleaved $\alpha_1$-antichymotrypsin did not polymerize and did not produce an increase in light scattering when incubated under the same conditions. Intrinsic tryptophan fluorescence has been used previously to assess the rate of polymerization of $\alpha_1$-antitrypsin (*13*, *14*, *34*). It was therefore assessed for its utility to monitor the polymerization of $\alpha_1$-antichymotrypsin. There was no change in intrinsic tryptophan fluorescence during polymer formation (data not shown). The free cysteine of $\alpha_1$-antichymotrypsin was therefore labeled with IANDB. Labeled $\alpha_1$-antichymotrypsin polymerized at the same rate as unlabeled protein when assessed by nondenaturing PAGE and light scatter (Figure 3c). The IANBD label reported a two-phase increase in fluorescence (Figure 3c) that was fitted to a double exponential model to calculate rate constants for

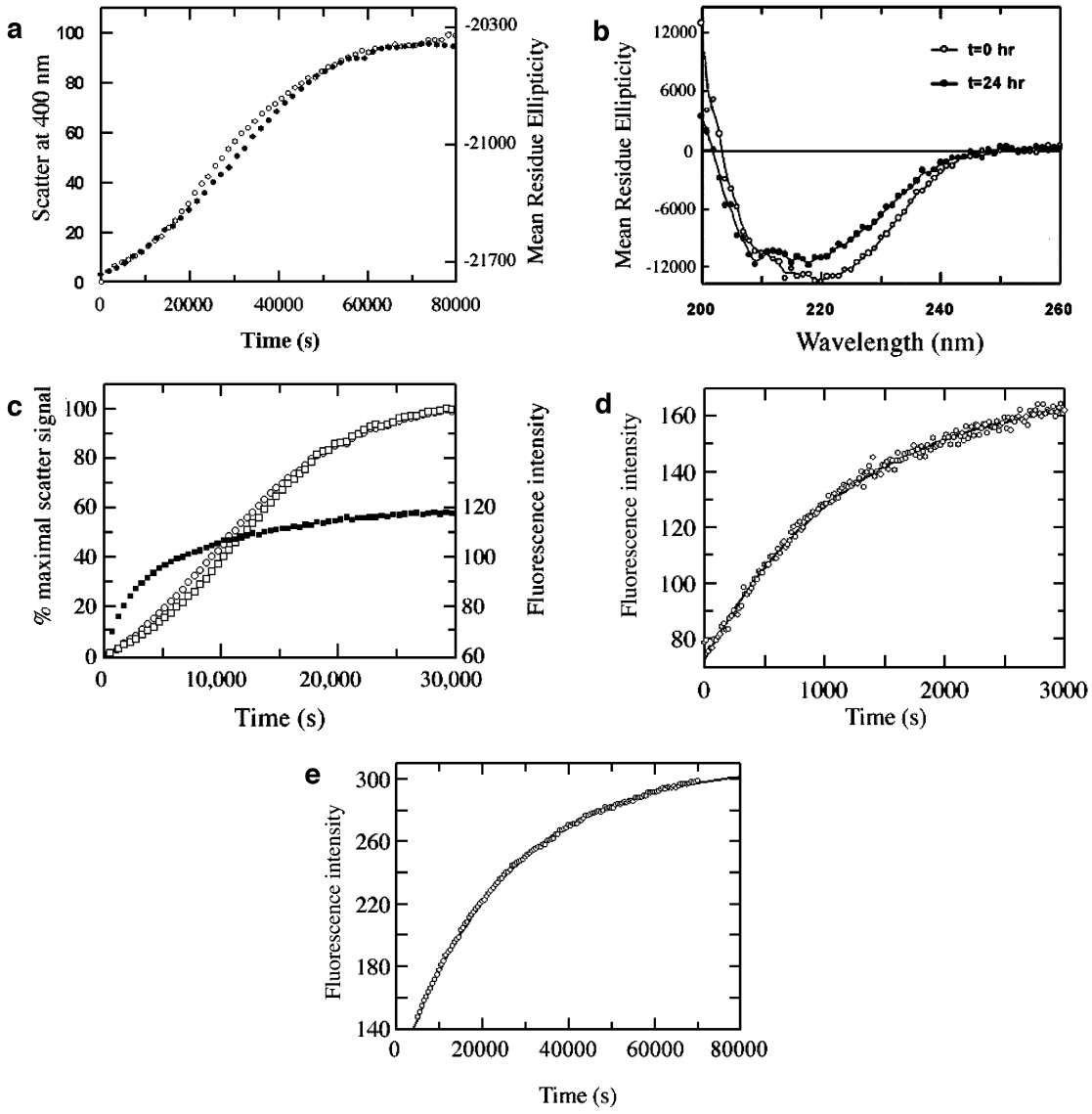


FIGURE 3: Spectroscopic assessment of $\alpha_1$-antichymotrypsin polymer formation. Polymerization of $\alpha_1$-antichymotrypsin was assessed by light scattering and CD spectroscopy. Native $\alpha_1$-antichymotrypsin was incubated at 45 °C and 200 $\mu$g/mL in 50 mM KCl and 50 mM Tris, pH 7.4. The increase in light scatter (open circles) closely paralleled the loss of CD at 222 nm (filled circles, expressed as mean residue ellipticity, degree·cm$^2$·dmole$^{-1}$·residue$^{-1}$) over 8 × 10$^4$ s (Figure 3a). Polymerization of $\alpha_1$-antichymotrypsin was accompanied by a loss of $\alpha$-helical structure and an increase in $\beta$-sheet structure content as determined by CD spectra before (Figure 3b, open circles) and after (Figure 3b, filled circles) incubation at 200 $\mu$g/mL and 45 °C in 50 mM KCl and 50 mM Tris, pH 7.4 for 24 h (expressed as mean residue ellipticity, degree·cm$^2$·dmole$^{-1}$·residue$^{-1}$). Fluorescence was also used to monitor the conformational changes of $\alpha_1$-antichymotrypsin during the polymerization reaction. The polymerization profiles (Figure 3c) of unlabeled (open circles) and IANDB-labeled (open squares) $\alpha_1$-antichymotrypsin were identical when assessed by light scattering at 400 nm. Labeled $\alpha_1$-antichymotrypsin gave a two phase increase in fluorescence (filled squares) during polymerization when excited at 478 nm and monitored at 541 nm. All proteins were incubated at 200 $\mu$g/mL in 50 mM Tris and 50 mM KCl, pH 7.4, at 45 °C. The fluorescence data were fitted to a double exponential model, enabling the determination of rate constants for the fast (Figure 3d) and slow (Figure 3e) components of the reaction.

the fast (Figure 3d) and slow (Figure 3e) components of the reaction. The rate constants were not related to the concentration of $\alpha_1$-antichymotrypsin, indicating that the IANBD label reports two unimolecular processes. The first-order rate constant for the fast component was 7.1 × 10$^{-4}$ s$^{-1}$ (95% confidence interval, 5.5−8.7 × 10$^{-4}$ s$^{-1}$) over a range of concentrations of $\alpha_1$-antichymotrypsin between 12.5 and 100 $\mu$g/mL. The first-order rate constant for the slow component was 3.5 × 10$^{-5}$ s$^{-1}$ (95% confidence interval 1.9−5.1 × 10$^{-5}$ s$^{-1}$) over a range of concentrations of $\alpha_1$-antichymotrypsin between 50 and 400 $\mu$g/mL. Blocking the $\beta$-sheet of $\alpha_1$-antichymotrypsin by insertion of a 12mer peptide corresponding to the reactive center loop of antithrombin abolished the increase in fluorescence recorded with the IANBD probe.

*Polymerization of $\alpha_1$-Antichymotrypsin Was Concentration and Temperature Dependent.* Polymerization reactions were performed over a range of concentrations of native $\alpha_1$-antichymotrypsin (100−400 $\mu$g/mL) at 45 °C (Figure 4a). They all demonstrated sigmoid scatter profiles with shorter lag times at higher protein concentrations. The polymerization reactions were also performed with 200 $\mu$g/mL native $\alpha_1$-antichymotrypsin at 42, 45, and 48 °C (Figure 4b). The scatter profiles also had shorter lag times at higher temperatures.

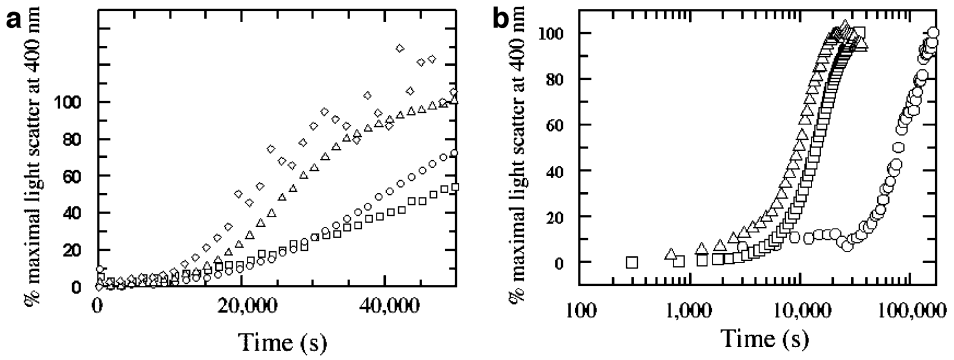


FIGURE 4: Rate of polymer formation was dependent on protein concentration and temperature. Native $\alpha_1$-antichymotrypsin (300 $\mu$L) was incubated at varying concentrations (100 $\mu$g/mL as squares, 200 $\mu$g/mL as circles, 300 $\mu$g/mL as triangles, and 400 $\mu$g/mL as diamonds) at 45 °C (Figure 4a) or varying temperatures (42 °C as circles, 45 °C as squares, and 48 °C as triangles) at 200 $\mu$g/mL (Figure 4b) in 50 mM KCl and 50 mM Tris, pH 7.4. Light scattering was measured at 400 nm. The profiles are representative of three independent experiments.

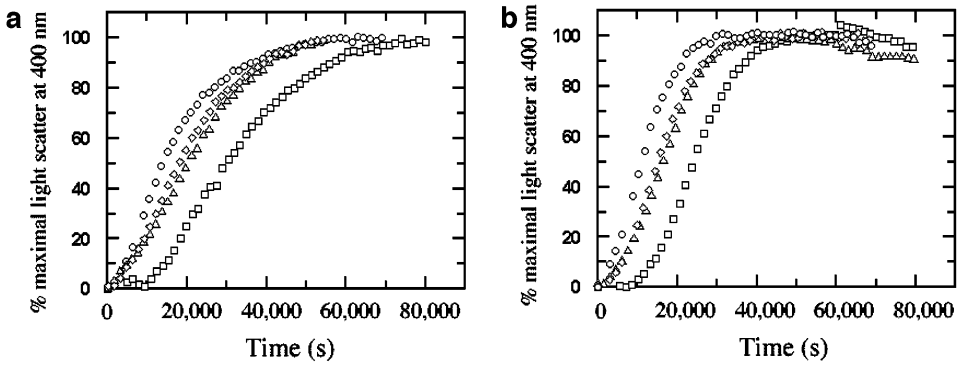


FIGURE 5: Effect of seeding with polymeric $\alpha_1$-antichymotrypsin on the polymerization of the native protein. Native $\alpha_1$-antichymotrypsin was incubated at 200 (Figure 5a) and 400 $\mu$g/mL (Figure 5b) at 45 °C in 50 mM Tris and 50 mM KCl, pH 7.4, in a final volume of 300 $\mu$L with the addition of 0 (squares), 2 (triangles), 6 (diamonds), and 20 $\mu$g (circles) of polymerized $\alpha_1$-antichymotrypsin (final concentration 0, 6.7, 20, and 66 $\mu$g/mL, respectively).

*Polymeric α1-Antichymotrypsin Specifically Seeds the Polymerization of Native Protein*. Polymers were formed by incubating native $\alpha_1$-antichymotrypsin at 200 $\mu$g/mL and 50 °C for 12 h and were confirmed by nondenaturing PAGE. The preformed polymers were then added in varying concentrations to solutions of monomeric $\alpha_1$-antichymotrypsin (200, 300, and 400 $\mu$g/mL in 50 mM Tris and 50 mM KCl, pH 7.4, at 45 °C), and the effect on the subsequent polymerization was assessed by light scattering (Figure 5a,b). The scatter profiles showed that the lag time for polymerization was reduced by the addition of polymeric $\alpha_1$-antichymotrypsin. The effect became more marked as increasing concentrations of polymer were added to the reaction mixture. The addition of polymeric $\alpha_1$-antichymotrypsin changed the profile of the scatter curve from sigmoid to hyperbolic indicating that polymeric $\alpha_1$-antichymotrypsin was able to seed the polymerization of monomeric protein. The effect of seeding with polymeric $\alpha_1$-antichymotrypsin was also assessed using IANBD labeled $\alpha_1$-antichymotrysin. The addition of polymers of unlabeled $\alpha_1$-antichymotrypsin to labeled native $\alpha_1$-antichymotrypsin did not change the rate constant for the fast or slow components of the fluorescence signal (data not shown).

*Seeding of α1-Antichymotrypsin Polymerization Is Serpin Dependent*. Alpha$_1$-antichymotrypsin polymers clearly accelerate the polymerization of native $\alpha_1$-antichymotrypsin. Polymers of other serpins were then assessed for their ability to induce polymerization. Neither polymers of $\alpha_1$-antitrypsin nor antithrombin at 100 $\mu$g/mL were able to accelerate the polymerization of native $\alpha_1$-antichymotrypsin in a standard light scatter assay (Figure 6). Short chain loop-sheet polymers of $\alpha_1$-antitrypsin prepared by heating plasma $\alpha_1$-antitrypsin in stabilizing concentrations of sodium citrate (*29*) were also unable to seed the polymerization of $\alpha_1$-antichymotrypsin (data not shown). Finally, the addition of an unrelated protein (100 $\mu$g/mL bovine serum albumin) to native $\alpha_1$-antichymotrypsin had no effect on the scatter profile (data not shown).

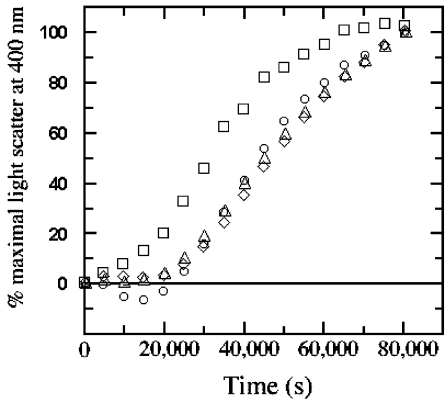


FIGURE 6: Alpha$_1$-antichymotrypsin polymers specifically accelerate the polymerization of native $\alpha_1$-antichymotrypsin. Native $\alpha_1$-antichymotrypsin was incubated at 200 $\mu$g/mL in 50 mM Tris and 50 mM KCl, pH 7.4, in the absence of polymeric serpin (diamonds) or in the presence of 100 $\mu$g/mL of $\alpha_1$-antitrypsin (triangles), antithrombin (circles), or $\alpha_1$-antichymotrypsin (squares) polymers. The rate of polymerization was assessed by light scattering at 400 nm. The profiles are representative of three independent experiments.

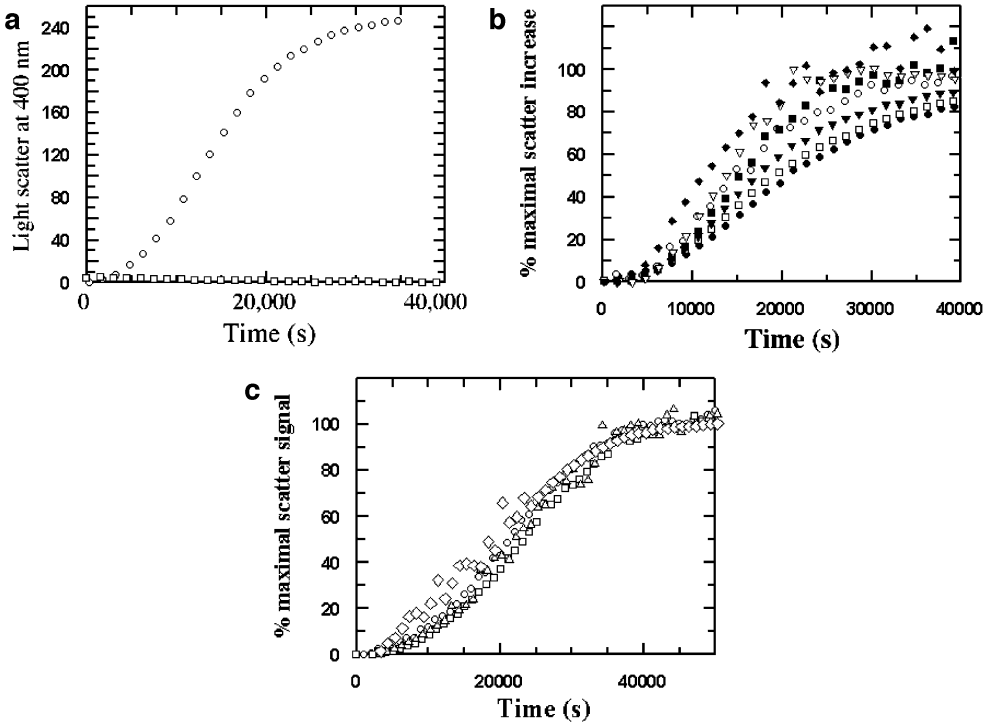


FIGURE 7: Effect of seeding with binary complexed $\alpha_1$-antichymotrypsin on the polymerization of the native protein. Binary complexed $\alpha_1$-antichymotrypsin did not polymerize when incubated on its own (Figure 7a, squares) in contrast to native $\alpha_1$-antichymotrypsin (circles). The binary complex caused a concentration dependent increase in the rate of polymerization of native $\alpha_1$-antichymotrypsin (Figure 7b) when 0 (filled circles), 3 (empty squares), 9 (filled triangles), 18 (empty circles), 24 (filled squares), 30 (empty triangles), or 36 $\mu$g (filled diamonds) were added. There was no acceleration of the rate of polymerization with reactive loop cleaved $\alpha_1$-antichymotrypsin (Figure 7c) when 0 (circles), 2 (squares), 6 (triangles), or 20 $\mu$g (diamonds) of cleaved $\alpha_1$-antichymotrypsin were added (final concentration 0, 6.7, 20, and 66 $\mu$g/mL, respectively). The profiles are representative of three independent experiments. Native $\alpha_1$-antichymotrypsin was at 200 $\mu$g/mL, and 300 $\mu$L incubations were performed in 50 mM Tris and 50 mM KCl, pH 7.4, at 45 °C.

*Serpin−Peptide Binary Complex Is the Minimal Seeding Species*. The loop-sheet model of serpin polymerization predicts that the reactive loop of one molecule of $\alpha_1$-antichymotrypsin will sequentially insert into $\beta$-sheet A of another (Figure 1b). One end of the $\alpha_1$-antichymotrypsin polymer must have a free reactive center loop, and this loop could act as a seed for further polymerization by inserting rapidly into $\beta$-sheet A of successive $\alpha_1$-antichymotrypsin monomers. The $\alpha_1$-antichymotrypsin-12mer peptide binary complex (Figure 1c) allowed us to determine whether increased exposure of the terminal reactive loop seeds polymerization. The binary complex is unable to accept the reactive loop from another molecule as $\beta$-sheet A is already filled by an exogenous peptide. It might however act as a supra-normal donor to facilitate polymer formation. The binary complex was therefore assessed for its ability to seed the polymerization of $\alpha_1$-antichymotrypsin. As expected, the $\alpha_1$-antichymotrypsin-12mer peptide binary complex alone did not undergo loop-sheet polymerization (Figure 7a). However, the binary complex accelerated the polymerization of $\alpha_1$-antichymotrypsin as determined by the standard light scatter assay (Figure 7b). The effect of the $\alpha_1$-antichymotrypsin-12mer peptide binary complex on the rate of polymerization did not result from contaminating polymeric $\alpha_1$-antichymotrypsin as silver stained gels of the binary complex showed no trace of $\alpha_1$-antichymotrypsin polymers. Reactive loop-cleaved $\alpha_1$-antichymotrypsin also has a complete six-stranded $\alpha_1$-sheet A but does not have an exposed reactive center loop (Figure 1d). Reactive loop cleaved $\alpha_1$-antichymotrypsin alone did not polymerize and gave no scatter signal. Moreover, reactive loop cleaved $\alpha_1$-antichymotrypsin was unable to accelerate the polymerization of native $\alpha_1$-antichymotrypsin (Figure 7c). This clearly demonstrates that the exposed reactive loop is essential to seed the polymerization of $\alpha_1$-antichymotrypsin.

*Seeding by Sonicated $\alpha_1$-Antichymotrypsin Polymers*. Polymeric $\alpha_1$-antichymotrypsin and $\alpha_1$-antichymotrypsin complexed with a reactive loop peptide were able to seed the polymerization of $\alpha_1$-antichymotrypsin, presumably by increasing the number of ends that are competent to act as a template for polymer formation. This model predicts that disrupted polymers should expose more end molecules and so accelerate polymerization. Alpha$_1$-antichymotrypsin polymers were formed by heating the protein at 200 $\mu$g/mL and 50 °C for 12 h. The polymers were disrupted by sonication and then used to seed polymerization. The data show that sonication of $\alpha_1$-antichymotrypsin polymers significantly increased their ability to seed polymerization of native $\alpha_1$-antichymotrypsin. There was a clear correlation between the duration of sonication and the potency of seeding (Figure 8). This effect was so marked that the disrupted polymers were able to seed $\alpha_1$-antichymotrypsin polymerization at 37 °C. Incubation of $\alpha_1$-antichymotrypsin alone under the same conditions at 37 °C did not result in the formation of polymers. Moreover, incubation of sonicated polymers alone did not cause an increase in signal, confirming that the effect was not simply because of the reassociation of disrupted polymers (data not shown).

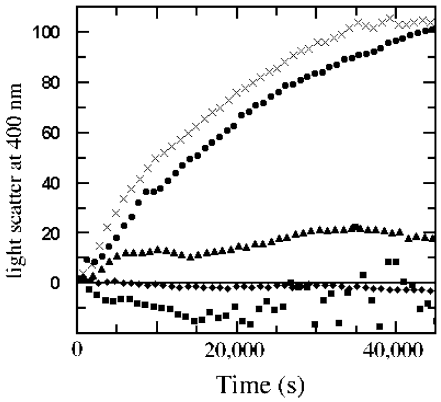


FIGURE 8: Sonication of $\alpha_1$-antichymotrypsin polymers increased the seeding of $\alpha_1$-antichymotrypsin polymerization. Native $\alpha_1$-antichymotrypsin was incubated at 200 $\mu$g/mL and 37 °C in a volume of 300 $\mu$L in the absence (diamonds) or presence of 20 $\mu$g of $\alpha_1$-antichymotrypsin polymers that had been sonicated for 0 (squares), 2 (triangles), 3 (circles), or 4 min (crosses). The rate of polymerization was assessed by light scattering at 400 nm. The profiles are representative of three independent experiments.

## DISCUSSION

Alpha$_1$-antichymotrypsin is an invariable component of the amyloid plaques in patients with Alzheimer's disease (*1*). The conformation of $\alpha_1$-antichymotrypsin within the plaque, the relationship with the A$\beta_{1-42}$ peptide, and the mechanism by which it is deposited are unclear. Previous studies have shown that $\alpha_1$-antichymotrypsin can both favor (*35*, *36*) and abrogate (*37*, *38*) the fibrillization of A$\beta_{1-42}$ depending on the concentration used in the assay. A$\beta_{1-42}$ has been shown to anneal to $\beta$-sheet A of $\alpha_1$-antichymotrypsin in vitro (*39*) and, despite the unknown significance of this interaction in vivo, there is a suggestion that polymerization of $\alpha_1$-antichymotrypsin is favored in patients with Alzheimer's disease as compared to controls (*40*). We report here the characterization of $\alpha_1$-antichymotrypsin polymerization.

Alpha$_1$-antichymotrypsin formed loop-sheet polymers that were similar to those of other members of the serpin superfamily (*23*, *32*, *41*). The polymers were visualized by nondenaturing PAGE and showed a characteristic high molecular mass ladder that failed to unfold in 8 M urea on a transverse urea gradient gel. Polymers were reduced to a monomeric conformation by heating with SDS and then were separated by SDS−PAGE. The appearance of polymers on the gels corresponded to an increase in light scattering at 400 nm. The interpretation of the signal from scatter assays requires caution as there is a complex nonlinear relationship between polymerization and light scatter. Fluorimetry was therefore used to support the validity of the scatter data. Intrinsic tryptophan fluorescence did not change during the polymerization reaction, and so the free cysteine on $\alpha_1$-antichymotrypsin was labeled with IANDB. The increase in fluorescence observed during an incubation of $\alpha_1$-antichymotrypsin at 45 °C was fitted to a double exponential model. Rate constants for the fast and slow components of the reaction were found to be independent of $\alpha_1$-antichymotrypsin concentration and hence reported only unimolecular conformational changes and not the polymerization reaction itself.

The polymerization process was also assessed by CD spectroscopy. There was a significant change at 222 nm that mirrored the profile observed with light scattering. This provides reassurance that light scatter is measuring polymerization as a consequence of a structural change in $\alpha_1$-antichymotrypsin and not merely nonspecific protein aggregation. The light scatter assay demonstrated that $\alpha_1$-antichymotrypsin polymerization was concentration and temperature dependent. This is similar to the findings with other serpins such as $\alpha_1$-antitrypsin and antithrombin (*13*). Indeed, the acute phase response and associated fever, which results in an increase in temperature and protein synthesis, have been proposed to accelerate polymer-mediated liver damage in patients with the Z mutation of $\alpha_1$-antitrypsin (*13*, *15*). Similarly, the well-documented up regulation of $\alpha_1$-antichymotrypsin in Alzheimer's disease (*1*, *42*−*47*) will increase the concentration of protein and predictably favor polymer formation.

The addition of preformed $\alpha_1$-antichymotrypsin polymers to monomeric $\alpha_1$-antichymotrypsin progressively abolished the initial lag phase in the light scatter profile during polymer formation. Moreover, the shape of the curve was transformed from sigmoidal to hyperbolic. This behavior is characteristic of a nucleation-dependent process and has never been previously described in polymerization of other members of the serpin superfamily (*13*, *15*, *21*, *32*, *33*). It resembles the mechanism of polymerization of $\beta$-amyloid (*2*) and $\alpha$-synuclein (*48*) in Alzheimer's and Parkinson's disease, respectively. To explain the mechanism by which $\alpha_1$-antichymotrypsin polymers accelerate the polymerization of the monomeric protein is important to consider the structure of the polymer (Figure 1b). The final molecule in a polymer chain must undergo a conformational change that makes it a more efficient acceptor or donor of reactive loops in the loop-sheet polymerization reaction. The binary complex of $\alpha_1$-antichymotrypsin with an exogenous reactive loop peptide was used to investigate whether the effect could be due to more efficient loop donation. The binary complex has a loop that may be expelled and available for donation but has a complete six-stranded $\beta$-sheet A (Figure 1c) and so cannot accept a reactive loop from another molecule of $\alpha_1$-antichymotrypsin. The inability of the binary complex of peptide and $\alpha_1$-antichymotrypsin to undergo polymerization strongly supports a model in which the reactive loop inserts as the fourth $\beta$ strand in $\beta$-sheet A rather than at other positions such as position seven as proposed for PAI-1 (*49*). The light scatter assay demonstrated a concentration dependent acceleration in $\alpha_1$-antichymotrypsin polymerization upon addition of binary complex. Cleaved $\alpha_1$-antichymotrypsin (Figure 1d) did not accelerate the polymerization reaction, demonstrating that completion of $\beta$-sheet A with a sixth strand was not in itself the cause of seeding.

The acceleration of polymerization was not a nonspecific effect of serpin polymers as neither short nor long chain polymers of $\alpha_1$-antitrypsin nor polymers of antithrombin were able to accelerate the polymerization of native $\alpha_1$-antichymotrypsin. Sonication of $\alpha_1$-antichymotrypsin polymers further increased the rate of native $\alpha_1$-antichymotrypsin polymerization supporting the hypothesis that it is the polymer end, probably the free-reactive loop end, that seeds the polymerization of the monomeric protein. This result was particularly striking as the sonicated $\alpha_1$-antichymotrypsin was able to accelerate polymerization of native $\alpha_1$-antichymotrypsin under physiological conditions and at body temper-

ature. These findings may well be important in the deposition of $\alpha_1$-antichymotrypsin in amyloid plaques in Alzheimer's disease, especially as there is an up-regulation of expression of $\alpha_1$-antichymotrypsin in the brains of patients with Alzheimer's disease.

## ACKNOWLEDGMENT

D.C.C. is a Wellcome Trust Intermediate Clinical Fellow, and L.C.S. is a Wellcome Trust Research Career Development Fellow. We would like to thank MRC Laboratory of Molecular Biology for the use of their electron microscope and Dr. Didier Belorgey, Cambridge Institute for Medical Research, for helpful discussion of the manuscript.

## REFERENCES

1. Abraham, C. R., Selkoe, D. J., and Potter, H. (1988) Immunochemical identification of the serine proteinase inhibitor $\alpha_1$-antichymotrypsin in the brain amyloid deposits of Alzheimer's disease, *Cell 52*, 487−501.
2. Harper, J. D., and Lansbury, P. T., Jr. (1997) Models of amyloid seeding in Alzheimer's disease and scrapie: Mechanistic truths and physiological consequences of the time-dependent solubility of amyloid proteins, *Annu. Rev. Biochem. 66*, 385−407.
3. Hartley, D. M., Walsh, D. M., Ye, C. P., Diehl, T., Vasquez, S., Vassilev, P. M., Teplow, D. B., and Selkoe, D. J. (1999) Protofibrillar intermediates of amyloid beta-protein induce acute electrophysiological changes and progressive neurotoxicity in cortical neurons, *J. Neurosci. 19*, 8876−84.
4. Conway, K. A., Lee, S. J., Rochet, J. C., Ding, T. T., Harper, J. D., Williamson, R. E., and Lansbury, P. T., Jr. (2000) Accelerated oligomerization by Parkinson's disease linked alpha-synuclein mutants, *Ann. N.Y. Acad. Sci. 920*, 42−5.
5. Conway, K. A., Lee, S. J., Rochet, J. C., Ding, T. T., Williamson, R. E., and Lansbury, P. T., Jr. (2000) Acceleration of oligomerization, not fibrillization, is a shared property of both alpha-synuclein mutations linked to early-onset Parkinson's disease: implications for pathogenesis and therapy, *Proc. Natl. Acad. Sci. U.S.A. 97*, 571−6.
6. Silverman, G. A., Bird, P. I., Carrell, R. W., Church, F. C., Coughlin, P. B., Gettins, P. G., Irving, J. A., Lomas, D. A., Luke, C. J., Moyer, R. W., Pemberton, P. A., Remold-O'Donnell, E., Salvesen, G. S., Travis, J., and Whisstock, J. C. (2001) The serpins are an expanding superfamily of structurally similar but functionally diverse proteins. Evolution, mechanism of inhibition, novel functions, and a revised nomenclature, *J. Biol. Chem. 276*, 33293−6.
7. Potempa, J., Korzus, E., and Travis, J. (1994) The serpin superfamily of proteinase inhibitors: structure, function, and regulation, *J. Biol. Chem. 269*, 15957−60.
8. Huber, R., and Carrell, R. W. (1989) Implications of the three-dimensional structure of $\alpha_1$-antitrypsin for structure and function of serpins, *Biochemistry 28*, 8951−66.
9. Huntington, J. A., Read, R. J., and Carrell, R. W. (2000) Structure of a serpin-protease complex shows inhibition by deformation, *Nature 407*, 923−6.
10. Mahadeva, R., and Lomas, D. A. (1998) Alpha$_1$-antitrypsin deficiency, cirrhosis and emphysema, *Thorax 53*, 501−5.
11. Stein, P. E., and Carrell, R. W. (1995) What do dysfunctional serpins tell us about molecular mobility and disease?, *Nature Struct. Biol. 2*, 96−113.
12. Elliott, P. R., Lomas, D. A., Carrell, R. W., and Abrahams, J.-P. (1996) Inhibitory conformation of the reactive loop of $\alpha_1$-antitrypsin, *Nature Struct. Biol. 3*, 676−81.
13. Dafforn, T. R., Mahadeva, R., Elliott, P. R., Sivasothy, P., and Lomas, D. A. (1999) A kinetic description of the polymerisation of $\alpha_1$-antitrypsin, *J. Biol. Chem. 274*, 9548−55.
14. Sivasothy, P., Dafforn, T. R., Gettins, P. G. W., and Lomas, D. A. (2000) Pathogenic $\alpha_1$-antitrypsin polymers are formed by reactive loop-$\beta$-sheet A linkage, *J. Biol. Chem. 275*, 33663−8.
15. Lomas, D. A., Evans, D. L., Finch, J. T., and Carrell, R. W. (1992) The mechanism of Z $\alpha_1$-antitrypsin accumulation in the liver, *Nature 357*, 605−7.
16. Elliott, P. R., Stein, P. E., Bilton, D., Carrell, R. W., and Lomas, D. A. (1996) Structural explanation for the dysfunction of S $\alpha_1$-antitrypsin, *Nature Struct. Biol. 3*, 910−1.
17. Mahadeva, R., Chang, W.-S. W., Dafforn, T., Oakley, D. J., Foreman, R. C., Calvin, J., Wight, D., and Lomas, D. A. (1999) Heteropolymerisation of S, I and Z $\alpha_1$-antitrypsin and liver cirrhosis, *J. Clin. Invest. 103*, 999−1006.
18. Gooptu, B., Hazes, B., Chang, W.-S. W., Dafforn, T. R., Carrell, R. W., Read, R., and Lomas, D. A. (2000) Inactive conformation of the serpin $\alpha_1$-antichymotrypsin indicates two stage insertion of the reactive loop; implications for inhibitory function and conformational disease, *Proc. Natl. Acad. Sci U.S.A. 97*, 67−72.
19. Aulak, K. S., Eldering, E., Hack, C. E., Lubbers, Y. P. T., Harrison, R. A., Mast, A., Cicardi, M., and Davis III, A. E. (1993) A hinge region mutation in C1-inhibitor (Ala$^{436}$→Thr) results in nonsubstrate-like behavior and in polymerization of the molecule, *J. Biol. Chem. 268*, 18088−94.
20. Eldering, E., Verpy, E., Roem, D., Meo, T., and Tosi, M. (1995) COOH-terminal substitutions in the serpin C1 inhibitor that cause loop overinsertion and subsequent multimerization, *J. Biol. Chem. 270*, 2579−87.
21. Bruce, D., Perry, D. J., Borg, J.-Y., Carrell, R. W., and Wardell, M. R. (1994) Thromboembolic disease due to thermolabile conformational changes of antithrombin Rouen VI (187 Asn→Asp), *J. Clin. Invest. 94*, 2265−74.
22. Lindo, V. S., Kakkar, V. V., Learmonth, M., Melissari, E., Zappacosta, F., Panico, M., and Morris, H. R. (1995) Antithrombin-TRI (Ala382 to Thr) causing severe thromboembolic tendency undergoes the S-to-R transition and is associated with a plasma-inactive high-molecular-weight complex of aggregated antithrombin, *Br. J. Haematol. 89*, 589−601.
23. Davis, R. L., Shrimpton, A. E., Holohan, P. D., Bradshaw, C., Feiglin, D., Sonderegger, P., Kinter, J., Becker, L. M., Lacbawan, F., Krasnewich, D., Muenke, M., Lawrence, D. A., Yerby, M. S., Shaw, C.-M., Gooptu, B., Elliott, P. R., Finch, J. T., Carrell, R. W., and Lomas, D. A. (1999) Familial dementia caused by polymerisation of mutant neuroserpin, *Nature 401*, 376−9.
24. Davis, R. L., Holohan, P. D., Shrimpton, A. E., Tatum, A., Daucher, J., Collins, G. H., Todd, R., Bradshaw, C., Kent, P., Feiglin, D., Rosenbaum, A., Yerby, M. S., Shaw, C.-M., Lacbawan, F., and Lawrence, D. A. (1999) Familial encephalopathy with neuroserpin inclusion bodies (FENIB), *Am. J. Pathol. 155*, 1901−13.
25. Davis, R. L., Shrimpton, A. E., Carrell, R. W., Lomas, D. A., Gerhard, L., Baumann, B., Lawrence, D. A., Yepes, M., Kim, T. S., Ghetti, B., Piccardo, P., Takao, M., Lacbawan, F., Muenke, M., Sifers, R. N., Bradshaw, C. B., Kent, P. F., Collins, G. H., Larocca, D., and Holohan, P. D. (2002) Association between conformational mutations in neuroserpin and onset and severity of dementia, *Lancet 359*, 2242−7.
26. Rubin, H., Plotnick, M., Wang, Z.-M., Liu, X., Zhong, Q., Schechter, M. N., and Cooperman, B. S. (1994) Conversion of $\alpha_1$-antichymotrypsin into a human neutrophil elastase inhibitor: demonstration of variants with different association rate constants, stoichiometries of inhibition, and complex stabilities, *Biochemistry 33*, 7627−33.
27. Lomas, D. A., Stone, S. R., Llewelyn-Jones, C., Keogan, M.-T., Wang, Z. M., Rubin, H., Carrell, R. W., and Stockley, R. A. (1995) The control of neutrophil chemotaxis by inhibitors of cathepsin G and chymotrypsin, *J. Biol. Chem. 270*, 23437−43.
28. Rubin, H., Wang, Z., Nickbarg, E. B., McLarney, S., Naidoo, N., Schoenberger, O. L., Johnson, J. L., and Cooperman, B. S. (1990) Cloning, expression purification, and biological activity of recombinant native and variant human $\alpha_1$-antichymotrypsins, *J. Biol. Chem. 265*, 1199−1207.
29. Lomas, D. A., Elliott, P. R., Chang, W.-S. W., Wardell, M. R., and Carrell, R. W. (1995) Preparation and characterisation of latent $\alpha_1$-antitrypsin, *J. Biol. Chem. 270*, 5282−8.
30. Lomas, D. A., Evans, D. L., Stone, S. R., Chang, W.-S. W., and Carrell, R. W. (1993) Effect of the Z mutation on the physical and inhibitory properties of $\alpha_1$-antitrypsin, *Biochemistry 32*, 500−8.
31. Morii, M., and Travis, J. (1983) Amino acid sequence at the reactive site of human $\alpha_1$-antichymotrypsin, *J. Biol. Chem. 258*, 12749−52.
32. Patston, P. A., Hauert, J., Michaud, M., and Schapira, M. (1995) Formation and properties of C1-inhibitor polymers, *FEBS Lett. 368*, 401−4.

33. Zhou, A., Faint, R., Charlton, P., Dafforn, T. R., Carrell, R. W., and Lomas, D. A. (2001) Polymerization of plasminogen activator inhibitor-1, *J. Biol. Chem. 276*, 9115−22.
34. Mahadeva, R., Dafforn, T. R., Carrell, R. W., and Lomas, D. A. (2002) 6-mer peptide selectively anneals to a pathogenic serpin conformation and blocks polymerization. Implications for the prevention of Z alpha(1)-antitrypsin-related cirrhosis, *J. Biol. Chem. 277*, 6771−4.
35. Ma, J., Yee, A., Brewer, H. B., Jr., and Potter, H. (1994) Amyloid-associated proteins $\alpha_1$-antichymotrypsin and apolipoprotein E promote assembly of Alzheimer $\beta$-protein into filaments, *Nature 372*, 92−4.
36. Janciauskiene, S., Eriksson, S., and Wright, H. T. (1996) A specific structural interaction of Alzheimer's peptide A$\beta_{1-42}$ with $\alpha_1$-antichymotrypsin stimulates amyloid fibril formation, *Nature Struct. Biol. 3*, 668−71.
37. Fraser, P. E., Nguyen, J. T., McLachlan, D. R., Abraham, C. R., and Kirschner, D. A. (1993) $\alpha_1$-antichymotrypsin binding to Alzheimer A$\beta$ peptides is sequence specific and induces fibril disaggregation in vitro, *J. Neurochem. 61*, 298−305.
38. Eriksson, S., Janciauskiene, S., and Lannfelt, L. (1995) $\alpha_1$-antichymotrypsin regulates Alzheimer $\beta$-amyloid peptide fibril formation, *Proc. Natl. Acad. Sci. U.S.A. 92*, 2313−7.
39. Janciauskiene, S., Rubin, H., Lukacs, C. M., and Wright, H. T. (1998) Alzheimer's peptide A$\beta_{1-42}$ binds to two $\beta$-sheets of $\alpha_1$-antichymotrypsin and transforms it from inhibitor to substrate, *J. Biol. Chem. 272*, 28360−4.
40. Licastro, F., Sirri, V., Trere, D., and Davis, L. J. (1997) Monomeric and polymeric forms of alpha-1 antichymotrypsin in sera from patients with probable late onset Alzheimer's disease, *Dement. Geriatr. Cogn. Disord. 8*, 337−42.
41. Lomas, D. A. (1994) Loop-sheet polymerisation: the structural basis of Z $\alpha_1$-antitrypsin accumulation in the liver, *Clin. Sci. 86*, 489−95.
42. Matsubara, E., Amari, M., Shoji, M., Harigaya, Y., Yamaguchi, H., Okamoto, K., and Hirai, S. (1989) Serum concentration of alpha 1-antichymotrypsin is elevated in patients with senile dementia of the Alzheimer type, *Prog. Clin. Biol. Res. 317*, 707−14.
43. Lieberman, J., Schleissner, L., Tachiki, K. H., and Kling, A. S. (1995) Serum alpha 1-antichymotrypsin level as a marker for Alzheimer-type dementia, *Neurobiol. Aging 16*, 747−53.
44. Licastro, F., Parnetti, L., Morini, M. C., Davis, L. J., Cucinotta, D., Gaiti, A., and Senin, U. (1995) Acute phase reactant alpha 1-antichymotrypsin is increased in cerebrospinal fluid and serum of patients with probable Alzheimer disease, *Alzheimer Dis. Assoc. Disord. 9*, 112−8.
45. Harigaya, Y., Shoji, M., Nakamura, T., Matsubara, E., Hosoda, K., and Hirai, S. (1995) Alpha 1-antichymotrypsin level in cerebrospinal fluid is closely associated with late onset Alzheimer's disease, *Intern. Med. 34*, 481−4.
46. Licastro, F., Davis, L. J., Polazzi, E., Rossi, S., and Cucinotta, D. (1996) Serological alpha 1-antichymotrypsin in patients with probable senile dementia of Alzheimer type: a short-term longitudinal study, *Alzheimer Dis. Assoc. Disord. 10*, 192−6.
47. Licastro, F., Pedrini, S., Ferri, C., Casadei, V., Govoni, M., Pession, A., Sciacca, F. L., Veglia, F., Annoni, G., Bonafe, M., Olivieri, F., Franceschi, C., and Edoardo Grimaldi, L. M. (2000) Gene polymorphism affecting alpha1-antichymotrypsin and interleukin-1 plasma levels increases Alzheimer's disease risk, *Ann. Neurol. 48*, 388−91.
48. Wood, S. J., Wypych, J., Steavenson, S., Louis, J. C., Citron, M., and Biere, A. L. (1999) alpha-synuclein fibrillogenesis is nucleation-dependent. Implications for the pathogenesis of Parkinson's disease, *J. Biol. Chem. 274*, 19509−12.
49. Sharp, A. M., Stein, P. E., Pannu, N. S., Carrell, R. W., Berkenpas, M. B., Ginsburg, D., Lawrence, D. A., and Read, R. J. (1999) The active conformation of plasminogen activator inhibitor 1, a target for drugs to control fibrinolysis and cell adhesion, *Structure 7*, 111−8.
50. Skinner, R., Chang, W.-S. W., Jin, L., Pei, X., Huntington, J. A., Abrahams, J.-P., Carrell, R. W., and Lomas, D. A. (1998) Implications for function and therapy of a 2.9 Å structure of binary-complexed antithrombin, *J. Mol. Biol. 283*, 9−14.
51. Loebermann, H., Tokuoka, R., Deisenhofer, J., and Huber, R. (1984) Human $\alpha_1$-proteinase inhibitor. Crystal structure analysis of two crystal modifications, molecular model and preliminary analysis of the implications for function, *J. Mol. Biol. 177*, 531−556.

BI0259305